HEAD ON HALL EFFECT SENSOR ARRANGEMENT FOR DISPLACEMENT MEASUREMENT

MICHAL KELEMEN[1], TATIANA KELEMENOVA[1], MARTIN VARGA[1], PETER JAN SINCAK[1], LUKAS LESTACH[1], ELENA SERGEEVNA BAYMETOVA[2], MARIA RAVILEVNA KOROLEVA[3], ALENA ALEKSEEVNA CHERNOVA[2]

[1]Technical University of Kosice, Faculty of Mechanical Engineering, Slovakia.

[2]Federal State Budget Educational Institution of Higher Education "Kalashnikov Izhevsk State Technical University", Russia,

[3]Federal State Budgetary Scientific Institution "Udmurt Federal Research Center of the Ural Branch of the Russian Academy of Sciences"

DOI: 10.17973/MMSJ.2021_10_2021026

e-mail to corresponding author: michal.kelemen@tuke.sk

ABSTRACT

Hall effect sensor is a very frequently used sensor in mechatronic products. There is little information in the catalogue sheets about the application possibilities of this type of sensor. This article examines the configuration options of this sensor and how to use it to achieve the best measurement uncertainty and minimal hysteresis.

KEYWORDS

Hall effect sensor, permanent magnet, measurement, uncertainty

1 INTRODUCTION

Hall effect sensors are sensitive to external magnetic fields and convert information about this magnetic field into an electrical signal. A change in the magnetic flux density of this sensor will cause a change in the Hall voltage at the output of this sensor. The external magnetic field is in most cases created by the magnetic field of the permanent magnet and the change in magnetic flux density is created by changing the relative position and distance of this permanent magnet from the sensor (Fig. 1).

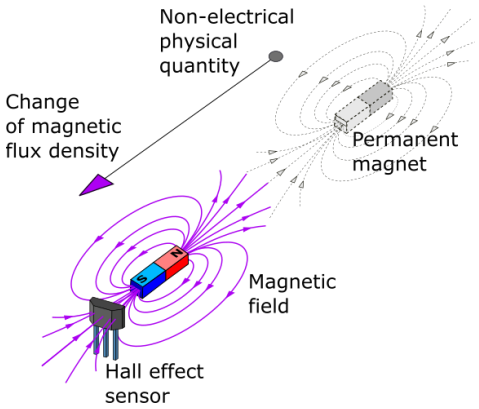

Figure 1. Hall effect sensor measurement principle

These sensors exist in two versions, with a digital output and linear sensors with an analogue output (Fig. 2).

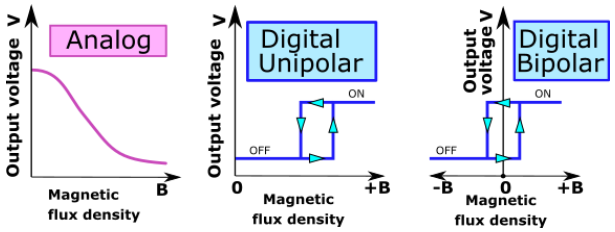

Figure 2. Output voltage for analog and digital type of Hall effect sensor

For linear encoders with analogue output, the value of the electrical voltage at the output changes in proportion to the magnetic flux density.

For sensors with a digital output, there is a Schmitt trigger inside, at the output of which the logic value changes rapidly from logic zero to a logic one (when the sensor is exposed in a magnetic field) and vice versa at a certain magnetic flux density. Thanks to the Schmitt trigger, digital sensors change their value abruptly without contact bounceless. Switching from logic zero to logic one is performed with built-in hysteresis to prevent oscillation of the output signal from the sensor as they move into the magnetic field and from the magnetic field. Digital sensors are therefore two-state, as they have only two possible states at their output. Depending on the polarity of the magnetic field to which these digital sensors respond, these sensors are manufactured in two versions, bipolar and unipolar. Bipolar digital sensors need a positive magnetic field (south pole) for their operation and a negative magnetic field (north pole) for their return to their original state. Unipolar digital sensors only need a magnetic south pole to activate and deactivate by moving into and out of the magnetic field.

From the point of view of their direct application, they provide at the output only a signal with a small value of electric current in the order of up to 20mA and for switching large current loads (large current loads) it is necessary to add, for example, an NPN transistor of the required power and possibly a relay or other switching element. The application of the sensor itself is then simple, because it is enough to add a permanent magnet to the moving sensed part of the system.

Hall effect sensors have been used extensively for one dimensional position analysis but their non-linear behaviour and cross-talk effects make them difficult to calibrate for effective and accurate two- and three-dimensional position and orientation analysis [Northey 2005].

A contactless linear displacement sensor for geotechnical purposes, using a new two-output CMOS Hall devise and a high-gradient permanent magnets actuating system, was experimentally tested [Roumenin 2007].

Authors of work [Addabbo 2018] discuss a low-cost distributed monitoring system for structural crack monitoring in monumental architecture. The proposed solution is suitable for monitoring widely extended areas like the Siena's ancient city walls. The prototype sensing system, based on Hall sensor technology, has been developed and characterized to reach a displacement resolution in the order of tens of micrometres [Addabbo 2018].

The aim of next study was to develop and calibrate a displacement measurement system for a hydraulic-actuation joystick used for repetitive motion analysis of heavy equipment operators. The system utilizes an array of four Hall effect sensors that are all active during any joystick movement [Northey 2006].

2 HALL EFFECT SENSOR AND PERMANENT MAGNET CONFIGURATIONS

The arrangement of the permanent magnet and the sensor can be realized in different configurations (Fig. 3) such as e.g. movement of the magnet towards the front of the sensor ("Head-on detection") where the magnetic field is perpendicular to the active surface of the sensor (Fig. 3a), lateral movement of the magnet to the sensor ("Sideways detection") where the magnet moves along the active surface of the sensor Fig. 3b), or other possibilities of their relative movement.

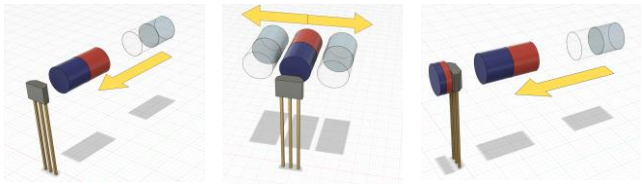

a) head on sensor arrangement | b) sideaway sensor arrangement | c) biasing magnet sensor arrangement

Figure 3. Basic configurations of sensor arrangement on the principle of hall effect and permanent magnet

With these possibilities of moving the magnet, it is also possible to change the polarity of the magnetic field of the magnet by rotating it, and so in total there are many configurations of how it is possible to use a sensor with a permanent magnet. Head-on detection is preferred when measuring the distance of the sensor from the magnet, and sideways detection is used to detect the presence of a magnetic field (for example, when registering a wheel rotation with a magnet attached to measure the speed of wheel rotation).

To detect the presence of ferromagnetic materials, it is possible to use a Hall effect sensor in a configuration with a small pre-magnetizing permanent magnet ("biasing magnet") located behind the active surface of the sensor (Fig. 3c). The sensor is thus in a constant magnetic field, and any change in the magnetic field caused by the presence of a ferromagnetic object will then be detected by this sensor.

3 APPLICATION POSSIBILITIES OF SENSORS ON THE PRINCIPLE OF HALL EFFECT

A change in the position of a permanent magnet can also be caused by another physical quantity (temperature, pressure, force, level, speed, or events that cause a change in the intensity of the magnetic field near the sensor. Hall effect sensors are popular due to their huge application possibilities in sensing position, speed and other physical quantities that can be sensed indirectly. Their attractiveness is mainly due to the fact that it is a non-contact sensing without wear of individual parts and so the life of these sensors is huge, and they are immune to dust, moisture and vibration and can be used in chemically aggressive and high risk of explosion and environments. with flammable substances. These sensors can operate at high switching speeds (several kHz) and can be used even at extremely low and high temperatures, while the sensors themselves do not contain any moving parts in their internal structure.

Probably the most massive area of application of these sensors are automotive systems, where the positions, distances and speeds of individual elements are sensed, such as crankshaft and camshaft position sensing for correct spark plugs control times, ignition distributor position with Hall effect sender, safety belt sensor, wheel speed sensor for anti-lock braking system (ABS), door and luggage compartment closing sensing, headlight rotation position sensing, transmission speed sensing in transmission sensor), acceleration pedal angle sensor, brake pedal angle sensor, Mirror sensor, fuel level sensor, Steering wheel rotation sensor for Active Stability Assist steering sensor, throttle position sensor for throttle position sensor), position sensing of windows, doors and dampers for in-vehicle climate control (HVAC), rotor position sensors for brushless electric motors (BLDC - brushless direct control motor rotor position sensor), car chassis position sensor for adaptive suspension system sensor, seat position detection sensor, water coolant valve sensor and many other applications for which no information is available [Abramov 2014, Beato-López 2019, Blanchard 2000, Hu 2020, Ivanova 2020, Kovac 2020, Mohankumar 2019, Northey 2006, Ripka 2019, Roumenin 2007, Sander 2014, Zhao 2015, Pavlasek 2018].

4 EXPERIMENTAL EXAMINATION OF HEAD ON SENSOR ARRANGEMENT CHARACTERISTICS

In this work, a sensor based on the Hall effect principle with an analogue ratiometric output was examined. The sensor type and manufacturer will not be specified due to GDPR. In this part, the behaviour of this sensor with different configurations of the sensor and magnet configuration is investigated (Fig. 4). These configurations have different permanent magnet application places and different permanent magnet polarities.

Head-on configurations H1 to H8 were used to examine the sensor (Fig. 4). Figure 4 shows all the possibilities of head-on configurations of the sensor on the principle of the Hall effect. Configurations H1, H2, H3 and H4 have a permanent magnet oriented perpendicular to the front or back surface of the sensor and the polarity of the permanent magnet changes. The H5 and H6 configurations have a permanent magnet perpendicular to the sensor head. Configurations H7 and H8 have a permanent magnet perpendicular to the side surface of the sensor.

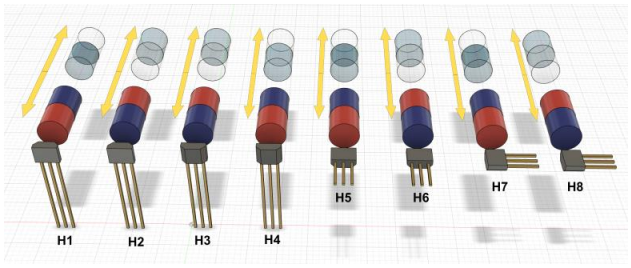

Figure 4. Head on sensor configurations based on the Hall effect principle with permanent magnets.

A stand with a positioning table (Fig. 5) was used for the experimental examination, where the sensor was placed on the fixed part of the stand and the permanent magnet was placed on the moving part. The mutual distance between the magnet and the sensor was set using a set of gauge length blocks. Ceramic length gauge blocks (Fig. 5) were used in this test so as not to affect the magnetic field of the permanent magnet. The process of changing the position of the permanent magnet relative to the sensor was solved in such a way that in the first stage of the measurement the permanent magnet first gradually moved away and then in the second stage the permanent magnet gradually approached the sensor. This method of measuring the response of a sensor to a change in position relative to a permanent magnet was used to determine the presence of hysteresis. The presence of hysteresis has an adverse effect on the application of the sensor.

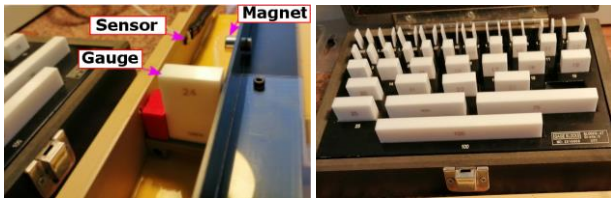

Figure 5. Measuring stand for examination of sensor properties on the principle of hall effect.

Three permanent magnets (Fig. 6) in the shape of a cylinder with a diameter of 10 mm and different lengths were selected for testing. Magnet 1 has a length of 10mm, magnet 2 has a length of 20mm and magnet 3 has a length of 30 mm. The magnet material is NdFeB with axial anisotropic polarization with remanence 1.25 T and coercive force 907 kA / m.

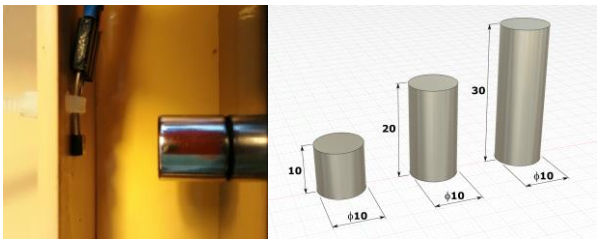

Figure 6. Location of permanent magnets and dimensions of permanent magnets used.

4.1 *Results of experiments for measuring using a permanent magnet with a diameter of 10 mm and a length of 10 mm*

Measurement configurations H1, H2, H3, H4 (Fig. 7a) have an area usable for position measurement in the range of the magnet position from the sensor from 8 mm to 30 mm. The configurations H5 and H6 (Fig. 7b) are unusable for measurement, because in these arrangements there were only minimal changes in the output voltage at the output of the sensor when the position of the permanent magnet relative to the sensor changed.

Configurations H7 and H8 (Fig. 7b) have a smaller usable range of position measurement in the range 0mm to 12mm compared to configurations H1 to H4.

Figure 7c shows a detail of the measured values for the configurations H1 to H4 and shows the phenomenon of hysteresis, which is more pronounced at the beginning of the interval. An enlarged view (Fig. 7d) shows that in the configuration H4 the phenomenon of hysteresis is the smallest and thus this configuration is the most advantageous from the point of view of the application for measurement.

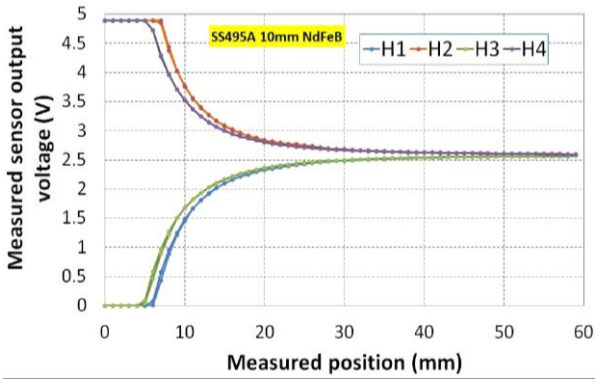

a)

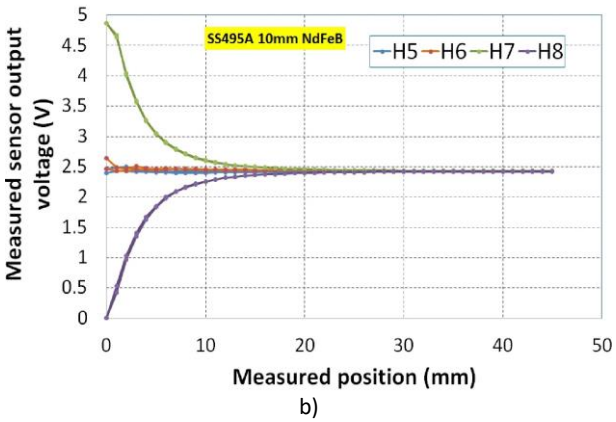

b)

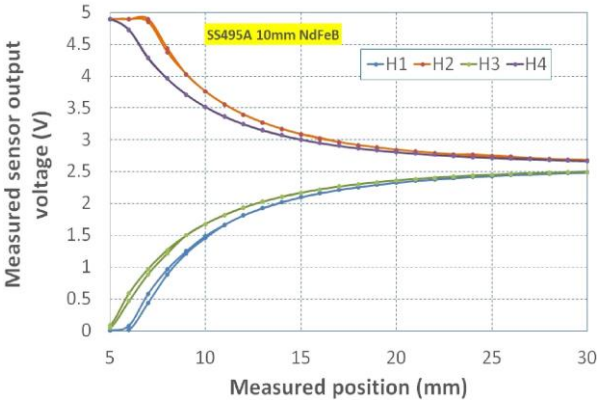

c)

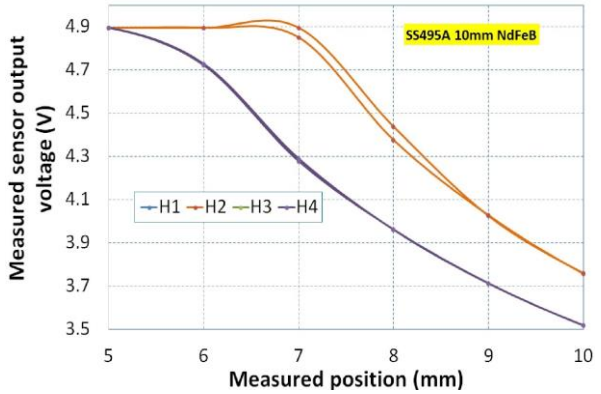

d)

Figure 7. Dependence of the output electrical voltage of the sensor on its position with respect to a cylindrical permanent magnet with a diameter of 10 mm and a length of 10 mm (a, b) and a detailed representation of the presence of hysteresis (c, d).

4.2 *Results of experiments for measuring using a permanent magnet with a diameter of 10 mm and a length of 20 mm*

When using a cylindrical permanent magnet with a diameter of 10 mm and a length of 20 mm, the results (Fig. 8a and b) are similar to the previous case. The detailed graphs (Fig. 8c and d) show the hysteresis again. The largest usable measuring range is for configurations H1 to H4. H5 and H6 configurations have results that are not usable for measurement purposes. With H7 and H8 configurations, this usable measurement area is smaller. Even in this case, the H4 configuration is the best in terms of the usability of this distance sensor, as it provides the largest measuring range with the least hysteresis.

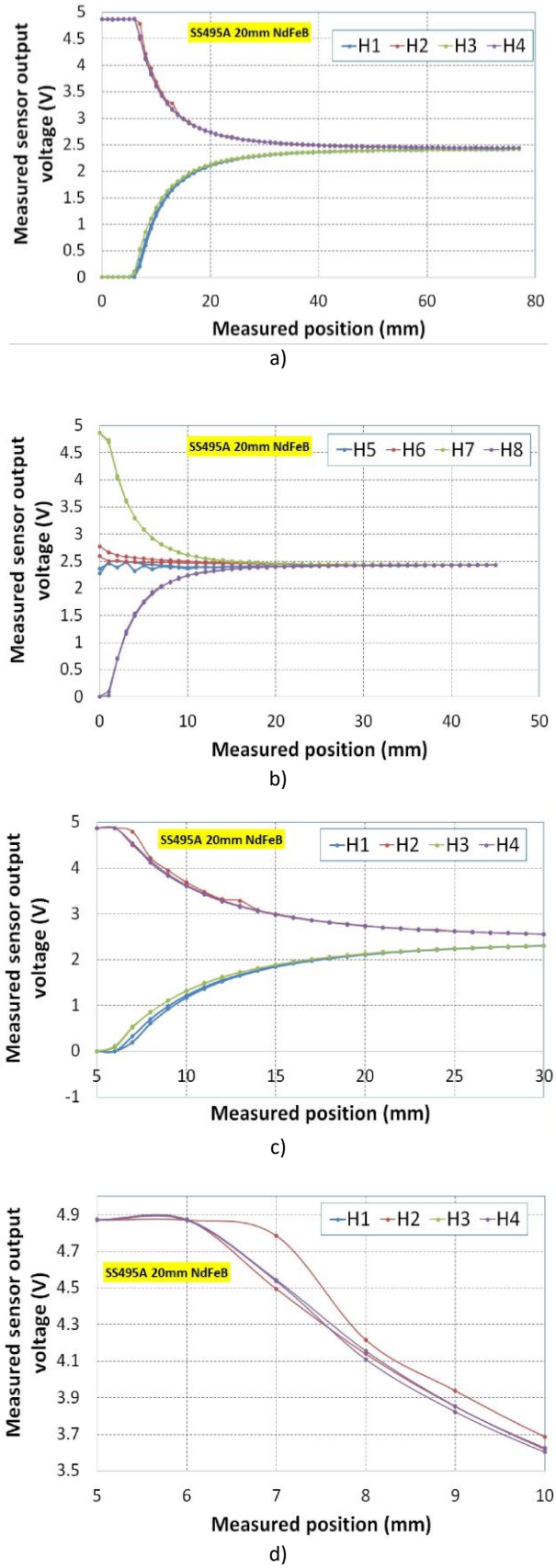

Figure 8. Dependence of the output electrical voltage of the sensor on its position with respect to a permanent magnet with a diameter of 10 mm and a length of 20 mm (a, b) and a detailed representation of the presence of the hysteresis phenomenon (c, d).

4.3 *Results of experiments for measuring using a permanent magnet with a diameter of 10 mm and a length of 30 mm*

The experiments were also performed for a cylindrical permanent magnet with a diameter of 10 mm and a length of 30 mm. The results (Fig. 9) were similar to previous cases (Fig. 8).

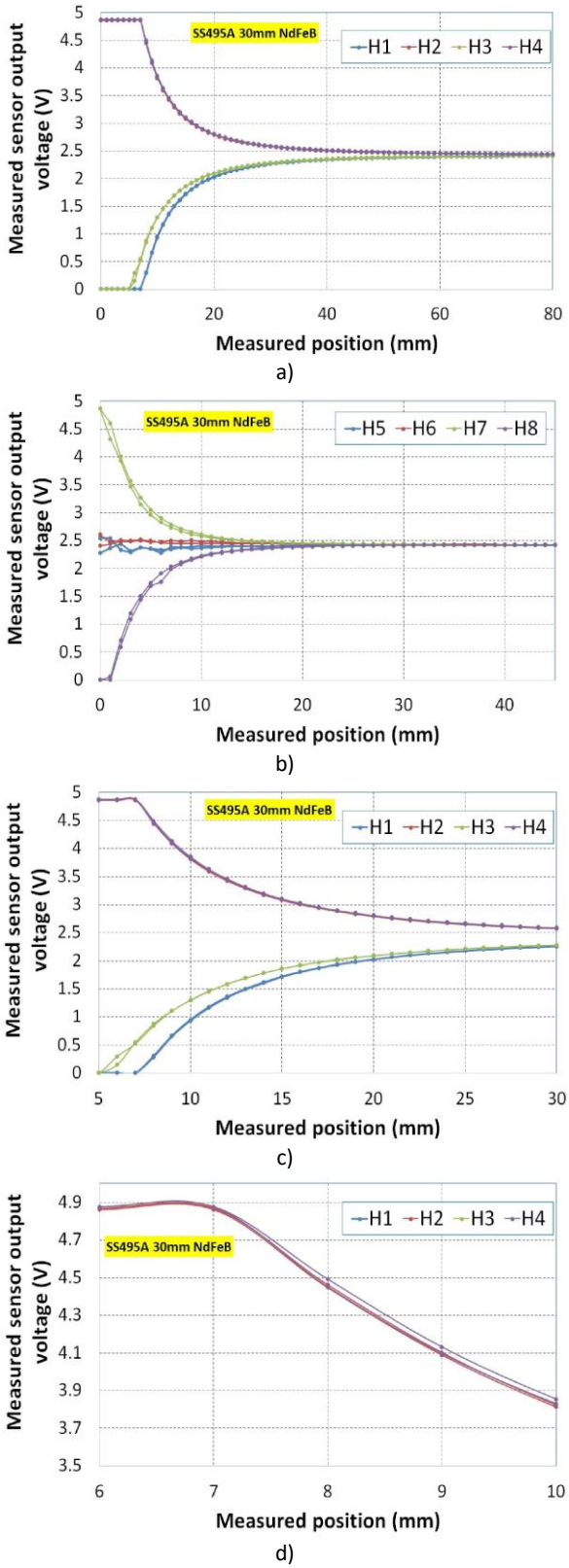

Figure 9. Dependence of the output electrical voltage of the sensor on its position with respect to a permanent magnet with a diameter of 10 mm and a length of 30 mm (a, b) and a detailed representation of the presence of the hysteresis phenomenon (c, d).

Also here, configurations H1 to H4 had the largest usable measuring range (Fig. 9a and b). The detailed graphs confirmed that even in this case, the most preferred arrangement is the H4 configuration (Fig. 9c and d). Configurations H7 and H8 have a smaller measuring range but have better sensitivity when measuring small distances, which is more advantageous for measuring of very small displacements.

5 DISCUSSION OF THE RESULTS

The results of the experiments showed that from the point of view of measurement, H4 (Fig. 10) is the most suitable configuration of the arrangement of the sensor and the permanent magnet. Three different lengths of cylindrical permanent magnet (10, 20 and 30 mm) were tested to determine the effect of permanent magnet length. The effect of different lengths of permanent magnets is shown in figure 10, the differences between them being negligible. This means that when using a particular cylindrical permanent magnet, increasing its length is unnecessary.

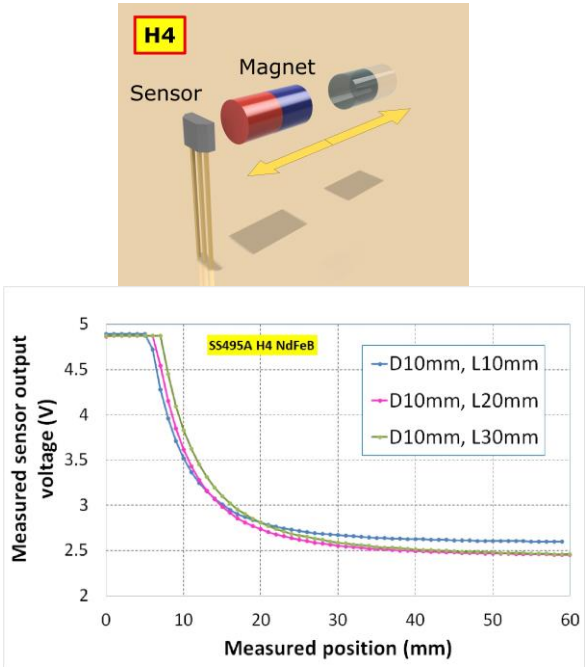

Figure 10. The most advantageous arrangement of the H4 sensor and the permanent magnet and the influence of different lengths of the permanent magnet on the output electrical voltage of the sensor.

6 CALIBRATION CHARACTERISTIC OF THE SENSOR MEASURING CHAIN FOR THE SELECTED CONFIGURATION

Regression analysis was performed for the selected configuration H4 with a permanent magnet with a length of 10 mm (Fig. 11), where different types of approximation functions were solved. From these functions, the most suitable is the polynomial function (Fig. 12), which was designed for a reduced measuring range. The obtained function can be used to recalculate the position of the magnet with respect to the sensor from the obtained value of the output electrical voltage of the sensor. In the case of using a computing device, e.g. microcontroller, it is possible to incorporate the obtained mathematical model (Fig. 12) directly into its program [Kayal 2005, Northey 2005].

To determine the stability of the sensor output voltage measurement data, repeated measurements were performed 100 times (Fig. 13) to determine whether the reading would not change over time under the same measurement conditions. How the scatter data around the mean is well described by the standard deviation.

Thus, in these measurements (Fig. 13), the standard deviations were processed by gradually adding values and recalculating other standard deviations. This means that with each new measurement value, a new standard deviation was calculated, which will provide us with information on how the standard deviation has changed with increasing new measurements (Fig. 14). Thus, this cumulative determination of the standard deviation gave us an answer to how many measurements need to be made in order to obtain the smallest possible standard deviation and the standard measurement uncertainty determined by method A. In addition, we have information on whether further repetition of the measurement is still important for improving the balance of measurement uncertainties.

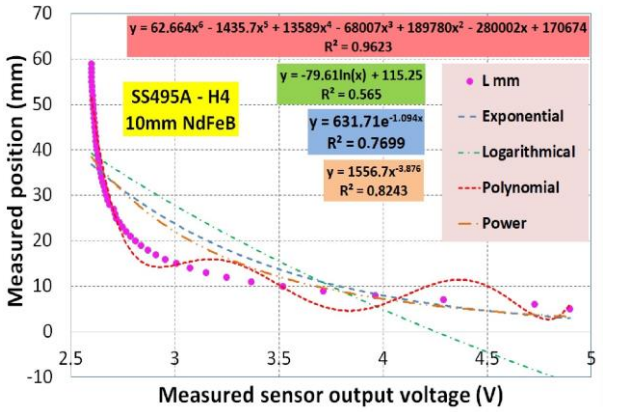

Figure 11. Regression analysis for the calibration characteristic of the tested sensor.

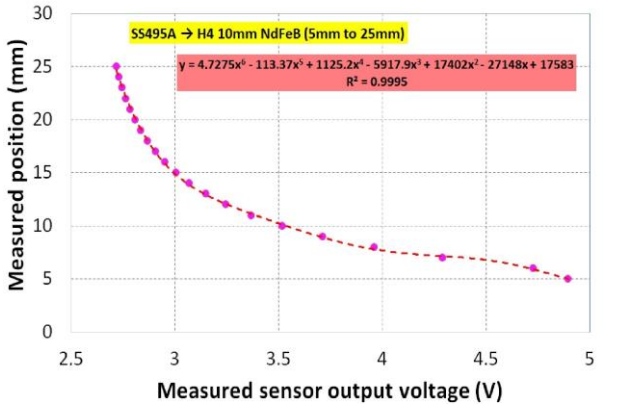

Figure 12. Approximation of the calibration characteristic using a polynomial function.

From the values measured at a distance of 10 mm (Fig. 14) are the worst values of standard deviations and so from these values the standard measurement uncertainties (Fig. 15) are determined depending on the number of performed measurements. The standard uncertainty determined by method B (Fig. 15) is determined from the catalogue sheet of the measuring instrument used. The standard measurement uncertainty determined by method A (Fig. 15) is determined from the values of standard deviations in the sense (EAL R2) and depends on the number of measurements performed. From the graph (Fig. 15) it is possible to observe a significant decrease in the standard uncertainty of measurement determined by method A, while after exceeding the number of measurements 20 the decrease of this value of uncertainty is only slight. Thus, the optimal number of measurements is 20 repetitions under the same measurement conditions.

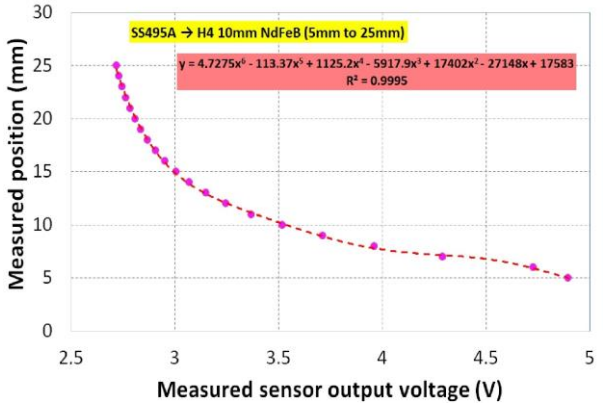

Figure 13. Repeated measurements for selected positions of the permanent magnet relative to the sensor.

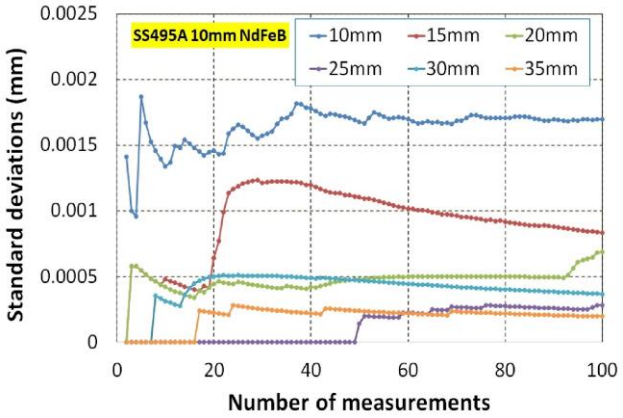

Figure 14. Cumulative standard deviation for repeated measures.

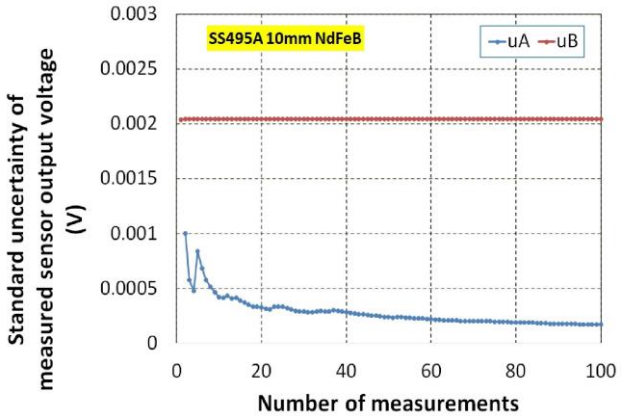

Figure 15. Standard uncertainty for measuring the output electrical voltage at the sensor output.

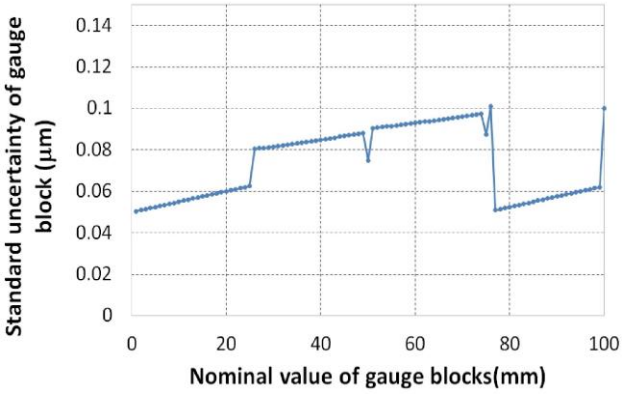

Figure 16. Standard uncertainty determined by Method B for scale block values used for calibration.

Ceramic gauge length blocks were used to set the distance between the permanent magnet and the sensor, each of which has a systematic error and uncertainty of nominal size defined by the manufacturer. According to these data, the uncertainties of the length standards composed of these gauge lengths were determined (Fig. 16).

7 CONCLUSION

In this work, a selected ratiometric hall effect sensor was tested using different head on configurations of the location of the permanent magnet H1 to H8. The results of the experiments show that the H4 configuration has the largest usable measuring range and at the same time minimal hysteresis. As a result, it is ideal for applications where it is necessary to measure the position of some objects. Furthermore, the effect of increasing the length of the magnet on the response of the sensor was observed, where it was found that the change in the length of the magnet has a negligible effect on the response of the sensor. For the H4 configuration with a permanent magnet with a length of 10 mm, a calibration characteristic was created, which was approximated by a polynomial model. This calibration characteristic can be used to calculate the measured position from the measured values of the output electrical voltage of the sensor. Furthermore, the influence of the number of measurements on the resulting measurement uncertainty was monitored, so that it was possible to determine the optimal number of measurements in terms of achieving the minimum measurement uncertainty and at the same time so that the number of measurements is not too large. The resulting measurement uncertainties showed that it is a very accurate position sensor and at the current price of this sensor, these results put it in the position of a very attractive sensor with a wide range of application options.

Future work will focus on exploring the sideaway sensor arrangement and biasing magnet sensor arrangement configurations. It will also seek to find the optimal configuration for measuring larger displacements above 50 mm. Furthermore, it will be necessary to solve the approximation of the experimental calibration characteristic using a suitable mathematical model for the purpose of implementation in a microcontroller for processing the measured data.

ACKNOWLEDGMENTS

The research was carried out with the financial support of Kalashnikov ISTU within the framework of the scientific project No. ЧАА/20-30-07. The authors would like to thank the Slovak Grant Agency—project KEGA 030TUKE-4/2020, VEGA 1/0201/21 and VEGA 1/0389/18. Authors also specially thank to supporting of project IVG-21-01 supported by the Faculty of Mechanical Engineering of Technical University of Kosice.

REFERENCES

[Abramov 2014] Abramov, I.V. Nikitin, Y.R., Abramov, A.I., Sosnovich, E.V., Bozek, P. Control and Diagnostic Model Of Brushless DC Motor. Journal of Electrical Engineering-Elektrotechnicky Casopis, 2014, Vol. 65, No. 5, pp. 277–282. DOI: 10.2478/jee-2014-0044.

[Addabbo 2018] Addabbo, T., Fort, A., Mugnaini, M., Panzardi, E., Pozzebon, A., Tani, M., Vignoli, V. A low cost distributed measurement system based on Hall effect sensors for structural crack monitoring in monumental architecture. Measurement. Volume 116, February 2018, Pages 652-657.

https://doi.org/10.1016/j.measurement.2017.11.050

[Beato-López 2019] Beato-López, J.J., Royo-Silvestre, I., Gómez-Polo, C. Micrometric non-contact position magnetoimpedance sensor. Journal of Magnetism and Magnetic Materials, 2018, Vol. 465, pp. 489–494. https://doi.org/10.1016/j.jmmm.2018.05.042

[Blanchard 2000] Blanchard, H., De Montmollin, F., Hubin, J., Popovic, R.S. Highly sensitive Hall sensor in CMOS technology. Sensors and Actuators, 2000, Vol. 82, pp. 144-148.

[Hu 2020] Hu, G., Zhang, H., Liu, Q. Review on sensors to measure control rod position for nuclear reactor. Annals of Nuclear Energy, 2020, Vol. 144, p. 107485. https://doi.org/10.1016/j.anucene.2020.107485

[Ivanova 2020] Ivanova, T.N., Bozek, P., Korshunov, A.I., Koretckiy, V.P. Control of the Technological Process of Drilling. MM Science Journal, 2020. DOI: 10.17973/MMSJ.2020_10_2020052.

[Kayal 2005] Kayal, M., Pastre, M. Automatic calibration of Hall sensor microsystems. Microelectronics Journal, 2006, Vol. 37, pp. 1569–1575. doi:10.1016/j.mejo.2006.04.013.

[Kovac 2020] Kovac, J., Svetlik, J., Rudy, V. Newest Development in Interconnecting the Data Cyber Glove 2 And The Robotic Hand Mechaterobot. MM Science Journal, 2020. DOI: 10.17973/MMSJ.2020_03_2019011.

[Mohankumar 2019] Mohankumar, P., Ajayan, J., Yasodharan, R., Devendran, P., Sambasivam, R. A review of micromachined sensors for automotive applications. Measurement, 2019, Vol. 140, pp. 305-322. https://doi.org/10.1016/j.measurement.2019.03.064.

[Northey 2006] Northey, G.W., Oliver M.L., Rittenhouse, D.M. Calibration of a Hall effect displacement measurement system for complex motion analysis using a neural network. Journal of Biomechanics, 2006, Vol. 39, pp. 1943–1947. doi:10.1016/j.jbiomech.2005.05.019.

[Olejarova 2016] Olejarova, S. Krenicky, T. Monitoring The Condition of the Spindle of the Milling Machine Using Vibration. MM Science Journal, 2016. DOI: 10.17973/MMSJ.2016_11_201653.

[Pavlasek 2018] Pavlasek, P., et al. Flexible Education Environment: Learning Style Insights to Increase Engineering Students Key Competences. In: EDULEARN18: 10th International Conference on Education and New Learning Technologies. Palma, Spain. Chova, L.G., Martinez, A.L., Torres, I.C. (Eds.). Book Series: EDULEARN Proceedings, pp. 10156-10165.

[Ripka 2019] Ripka, P., Mirzaei, M., Chirtsov, A., Vyhnanek, J. Transformer position sensor for a pneumatic cylinder. Sensors and Actuators A, 2019, Vol. 294, pp. 91–101. doi.org/10.1016/j.sna.2019.04.046.

[Roumenin 2007] Roumenin, Ch.S., Lozanova, S.V. Linear displacement sensor using a new CMOS double-hall device. Sensors and Actuators A, 2007, Vol. 138, pp. 37-43. doi:10.1016/j.sna.2007.04.042

[Sander 2014] Sander, C., Vecchi, M.C., Cornils, M., Paul, O. Ultra-Low Offset Vertical Hall Sensor in CMOS Technology. Procedia Engineering, 2014, Vol. 87, pp. 732-735.

[Zhao 2015] Zhao, B., Wang, L., Tan, J.B. Design and Realization of a Three Degrees of Freedom Displacement Measurement System Composed of Hall Sensors Based on Magnetic Field Fitting by an Elliptic Function. Sensors, 2015, Vol. 15, pp. 22530-22546; doi:10.3390/s150922530.

CONTACTS:

Michal Kelemen, Prof. Ing. PhD.
Technical University of Kosice, Faculty of Mechanical Engineering,
Institute of Automation, Mechatronics, Robotics and Production Techniques,
Letna 9, 04200 Kosice, Slovak Republic
michal.kelemen@tuke.sk